Saturated output of a Ge XXIII x-ray laser at 19.6 nm

J. Zhang,[1] P. J. Warwick,[2] E. Wolfrum,[3] M. H. Key,[1,3] C. Danson,[3] A. Demir,[4] S. Healy,[5] D. H. Kalantar,[6] N. S. Kim,[1] C. L. S. Lewis,[2] J. Lin,[4] A. G. MacPhee,[2] D. Neely,[3] J. Nilsen,[6] G. J. Pert,[5] R. Smith,[4] G. J. Tallents,[4] and J. S. Wark[1]

[1]*Clarendon Laboratory, Department of Physics, University of Oxford, Oxford, OX1 3PU, United Kingdom*
[2]*School of Mathematics and Physics, Queen's University of Belfast, Belfast, BT7 1NN, United Kingdom*
[3]*Central Laser Facility, Rutherford Appleton Laboratory, Chilton, Oxon, OX11 0QX, United Kingdom*
[4]*Department of Physics, University of Essex, Colchester, CO4 3SQ, United Kingdom*
[5]*Department of Computational Physics, University of York, York, YO1 5DD, United Kingdom*
[6]*Lawrence Livermore National Laboratory, Livermore, California 94550*

(Received 8 July 1996)

We report on measurements of the saturated single frequency output of a Ge XXIII x-ray laser on the $J=0\rightarrow1$ transition at 19.6 nm from a refraction compensating double target driven by 150 J of energy from 75-ps Nd-glass laser pulses. The 19.6-nm line completely dominated the laser output. The output energy was measured to be 0.9 mJ in a beam of 6.6×30 mrad^2 divergence, corresponding to a conversion efficiency of 6×10^{-6}. [S1050-2947(96)51012-7]

PACS number(s): 42.60.By, 32.30.Rj, 32.70.−n, 52.50.Jm

X-ray lasers from laser-produced plasmas have been demonstrated in Ne-like ions ranging from chlorine ($Z=17$) to silver ($Z=47$) [1,2]. Saturation has been observed on $J=2\rightarrow1$ transitions in Ge [3], Se [4], and Y [5] plasmas and on the $J=0\rightarrow1$ transition on Zn plasma [6]. Saturated operation is very important because it means that the maximum power possible for a given volume of an excited plasma is extracted by stimulated emission. Saturation also tends to produce an output energy sufficient for applications and ensures the production of a consistent output with little variation from shot to shot. Such consistent saturated output on a single laser line is needed for applications such as interferometry [7], but it has previously been observed mostly on $J=2\rightarrow1$ transitions, which typically generate a doublet of lines with comparable intensities.

X-ray lasers on $J=0\rightarrow1$ transitions are especially interesting as they generate a single wavelength. Recently, saturation has been demonstrated on the $J=0\rightarrow1$ transition at 21.2 nm in a Zn plasma using a prepulse technique [6]. The prepulse heats, ionizes, and expands the plasma. Between pulses, the plasma cools down and is not as transparent to the optical drive laser, and the lasing region of the plasma can directly absorb energy from the main pulse. A larger, more uniform density plasma at the densities required for the $J=0\rightarrow1$ gain is then generated during the main pulse [8,9]. The much reduced density gradient allows the $J=0\rightarrow1$ x-ray laser beam to propagate a longer distance at higher density along the excited plasma column and therefore obtains sufficient amplification for saturation to occur.

We are interested here particularly in a saturated laser on the 19.6-nm $J=0\rightarrow1$ transition. One application of such a laser is the study of the hydrodynamic imprinting of a laser speckle pattern on directly driven laser fusion targets [10]. More generally, the 19.6-nm wavelength is also just on the long side of the Al L edge, which has a high transmission at this wavelength and allows discrimination against stray light. In order to provide information of the fast evolving plasmas and to reduce blurring due to the hydrodynamic motion of the plasma, it is preferable to have an x-ray laser pulse duration of less than 100 ps. It has been demonstrated that it is possible to produce a 50-ps laser pulse at 19.6 nm with multiple 100-ps drive pulses while maintaining a high output energy [11].

The experimental setup is shown in Fig. 1. Six beams of the Vulcan glass laser with a 75-ps duration at 1.05 μm were used in a standard off-axis focus geometry, where $f/2.5$ spherical lenses focused three beams from one side of the target chamber to a spot focus that was then imaged by $f/2.5$ off-axis spherical mirrors to produce a line focus 25 mm long and 100 μm wide. The total energy on the line focus was about 75 J after a 20% reflection and transportation loss by the relay and focusing system, giving an irradiance of $\sim4\times10^{13}$ W cm^{-2} on target. Deploying the other three beams 180° opposed in a second line focus produced a plasma with an opposed density gradient that compensates for refractive deviation of the x-ray laser beam from the first plasma [3].

A prepulse was introduced by splitting the oscillator pulse into two pulses before the preamplifiers in the Vulcan laser. A variable prepulse between 10% and 30% of the total en-

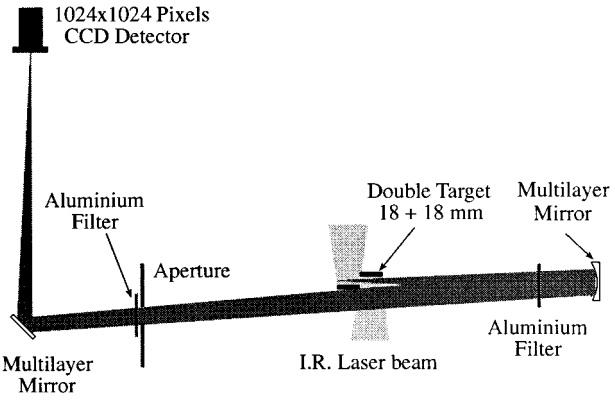

FIG. 1. Schematic of the experimental setup.

ergy on target was produced and delivered 2.2 ns in advance of the main pulse. The prepulse level and pulse duration were monitored by a fast photodiode system and an optical streak camera.

The slab targets used in the experiment were 18-mm-long 100-μm-wide Ge stripes coated on glass substrates. Both ends of the slab targets were placed well within the line focus to avoid cold plasmas at the ends of the targets. The targets were prealigned in a double target mount so that they were parallel with an adjustable separation (in a direction perpendicular to the target surfaces) between the surface planes and an axial separation of 500 μm between the two targets. Since the x-ray laser pulse duration is comparable to the propagation time, traveling-wave excitation for the two successive targets was used to optimize amplification; i.e., the three drive beams for the first slab target were timed 60 ps earlier than the three beams for the second target. The targets were aligned relative to the target chamber axis using a magnifying charge-coupled-device (CCD) system to accuracies of ± 1 mrad and ± 5 μm.

In order to measure the output energy of the $J=0\rightarrow 1$ laser, a standard beam imaging diagnostic was used consisting of multilayer mirrors [12], Al filters, and a Peltier cooled back thinned x-ray CCD detector with 1024×1024 pixels and 24-μm pixel size, as shown schematically in Fig. 1. The mirrors had superpolished ($<$0.1-nm rms roughness) substrates and were coated with 30-layer pairs of Mo and Si. They had a measured peak reflectivity of about 20% at a central wavelength of 19.6 nm with a full width at half maximum (FWHM) bandwidth of 1.5 nm. The concave multilayer mirror had 50-cm focal length and was positioned to image the output end of the Ge x-ray laser via a 45° planar multilayer mirror onto the CCD detector at a magnification of 16×. For some shots, a plane 3.0 cm from the laser output end was imaged to provide quasi-far-field information.

The imaging system was calibrated by placing at the imaging plane a grid target with fine bars repeated each 25 μm. Analysis of this image showed the resolution of the system to be better than 5 μm and calibrated the magnification at 16×. The imaging mirror had an aperture of about 25 mm, which gave an acceptance solid angle of 2.5×10^{-3} sr (50 mrad in both the horizontal and vertical directions). Astigmatism in the image was minimized by operating the imaging mirror at less than 0.6° off normal incidence. The planar mirror and the apertures in the path provided screening against broadband thermal x-ray emission. The aluminum filters protected against stray laser light and attenuated the x-ray laser beam.

The reflectivity of each multilayer mirror and the transmission of each filter were calibrated using x-ray radiation from a laser-produced plasma source coupled to a grating spectrometer [13]. The transmission of a 3.2-μm-thick Al filter was measured to be $9\pm 2\times 10^{-4}$, which agrees reasonably with the calculated value using Henke data [14]. The total response of the system provides a high rejection outside the 1.5-nm bandpass of the multilayer mirrors. The total uncertainty of the transmission is estimated to be a factor of 1.5. For some shots, the multilayer mirrors were replaced by two axial flat-field grating spectrometers to give an independent measurement of angular distribution and the output energy of the x-ray laser from both ends of the laser plasma.

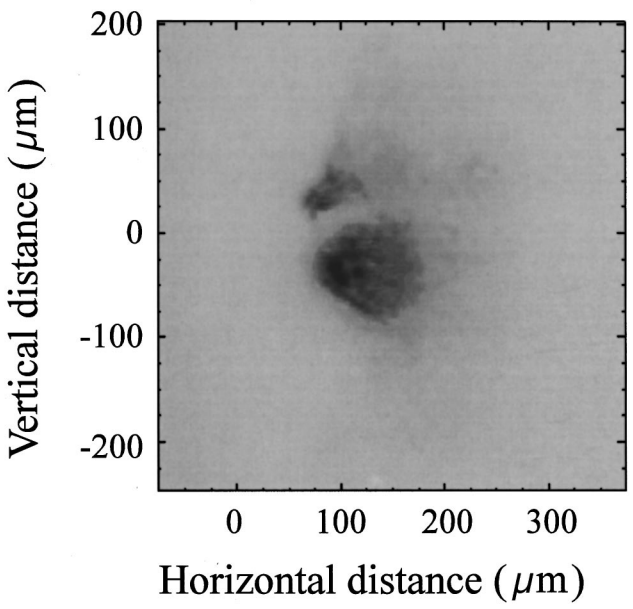

FIG. 2. Near-field image of the Ge XXIII laser from a double target with a 200-μm perpendicular separation.

Off-axis diagonstics included two spatially resolved crystal spectrometers coupled to InstaSpec VI x-ray CCD detectors (Orial Instrument, Stratford, CT). Resonance emission from the Ne-like and F-like ionization stages in the wavelength range of 7.0–10.5 Å from the two opposing germanium plasmas was monitored to provide information on ionization balance and the uniformity of the plasmas. The ratio between the F-like and Ne-like resonance lines gives a very sensitive monitoring of the uniformity of the illumination on target.

Figures 2 and 3 show a near-field and a quasi-far-field image (at 3 cm from the exit plane), respectively, of the Ge x-ray laser from the double target with a perpendicular separation of 200 μm between the planes of the two targets. This perpendicular direction is the horizontal axis in the figures with zero corresponding to the original target surface. The target surface position was determined using the integral thermal emission from the target surface. The characteristic two-lobe structure was observed at the near field of a single slab target, as predicted by theory [15] and observed in other experiments [12,16]. For the double-target configuration, an asymmetric distribution in brightness was observed in the parallel direction both in the near- and far-field images. This is believed to be due to asymmetric amplification caused by a small mismatch of the opposing plasmas in the direction parallel to the target surface [17]. Comparing the near- and far-field images, the x-ray photons spread over a much wider angle in the parallel direction than those in the perpendicular direction. This is plausible since the output characteristics of the laser beam are mainly determined by propagation through the two opposing plasmas, and both the opposing plasmas and the prepulse improve the propagation process only in the perpendicular direction. After a propagation of 3 cm distance, the divergence in the perpendicular direction is only 6.6 mrad. This result agrees with the measurements of angular distribution using on-axis spectrometers. The divergence in the parallel direction was measured to be as large as

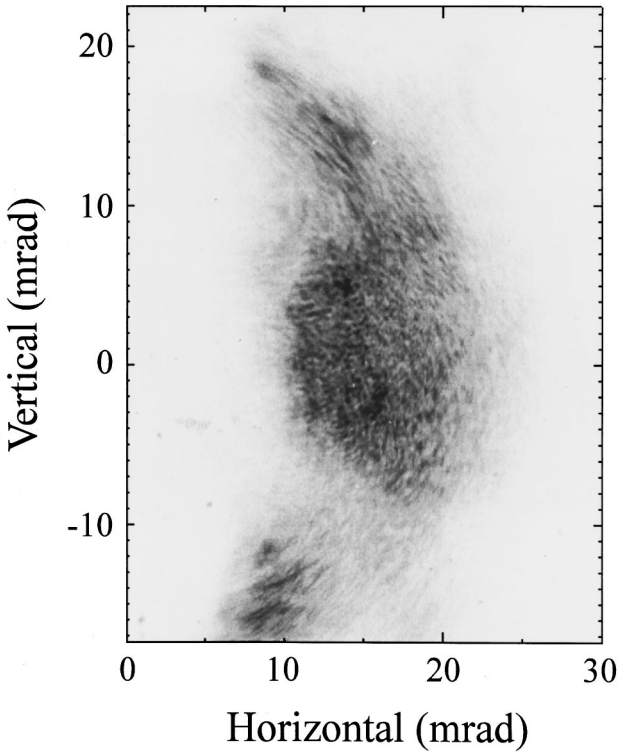

FIG. 3. Image of the x-ray laser beam 3 cm from the output plane for a double target with 200-μm perpendicular separation.

30.4 mrad, which was the combined effect of the propagation through the two plasmas. This divergence is also significantly larger than that of the Ge $J=2\rightarrow1$ laser [12], because the $J=0\rightarrow1$ laser generated from a higher density region [8,9].

Since the collection solid angle of the imaging mirror system exceeds that of the Ge laser beam, the output energy can be estimated by integrating the total photons emitted from the gain region and using an absolute calibration for the CCD detector and the calibrations for the x-ray multilayer mirrors and Al filters. The output energy of the Ge laser for an optimized separation (200 μm) between the two targets was estimated to be $\sim$0.9 mJ, indicating operation well into the saturated output regime, corresponding to an energy conversion efficiency of 6×10^{-6}.

In Fig. 4 the variation of the output energy against the perpendicular separation between the two targets is shown. The solid triangles with solid line show the measured output energy collected by the imaging mirror. The solid squares represent the measurements using an axial flat-field grating spectrometer, based on the calibration of the grating (5% reflection at 19.6 nm) and the double-reflection filter in front of the grating (5% reflection). The spectrometer has a collection angle of 46 mrad in the perpendicular direction, large enough to collect all the photons from the Ge laser in that direction. But the parallel collection angle of the spectrometer is only 13 mrad, 2.3 times smaller than the divergence angle of the x-ray laser beam. This is therefore taken into account in our estimate. It should be noted that the measurement using an axial flat-field grating spectrometer in Fig. 4 was obtained from a slightly different pulse configuration in which two prepulses separated by 400 ps were used 2.2 ns before the main pulse. The measurements were then normalized with the measurements, using a single prepulse presented here [18]. Both measurements show a strong coupling effect at a perpendicular separation around 200 μm.

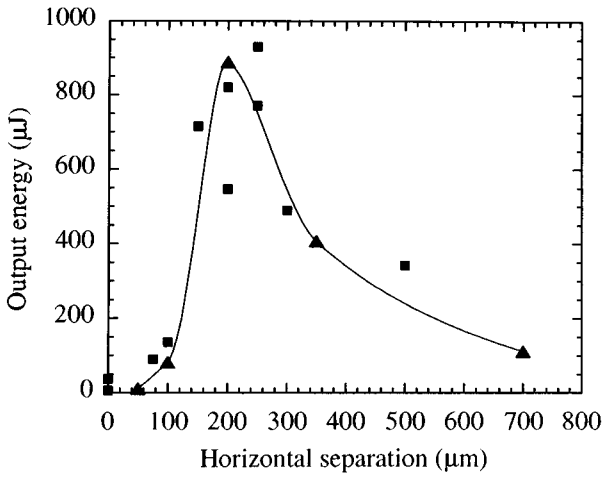

FIG. 4. Output energy of the Ge XXII laser vs perpendicular separation between the target surface planes.

It is striking from the axial spectrum (Fig. 5) that the Ge $J=0\rightarrow1$ line completely dominates the laser output, as predicted by theories. The other $J=2\rightarrow1$ laser lines at 23.2 and 23.6 nm are much weaker by a factor of over three orders of magnitude. The gain duration was not measured, but previous experiments indicated that the Ge x-ray laser pulse duration driven by multiple 100-ps pulses is about half of the drive pulse duration [11]. If we make a similar assumption for these experiments (as indicated by simulations under our experimental conditions [19]), the peak x-ray laser output power is therefore estimated to be 22 MW. It should be noted that the measurements in Ref. [11] were carried out with a single slab target driven by a traveling-wave excitation. The measurements presented here were made with a double slab target driven by a traveling-wave excitation approximated by delaying (by a time required by a laser photon traveling from the first slab to the second) the irradiation of the second slab target. Nevertheless, the data in Fig. 4 clearly show a strong increase in output when the perpendicular separation of the target is optimized. This confirms that the

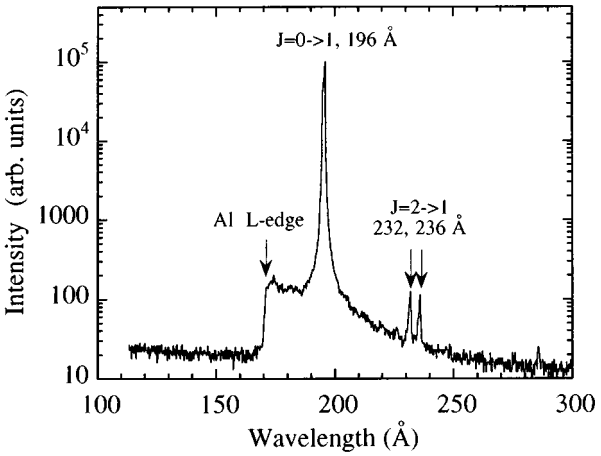

FIG. 5. Axial spectrum showing that the 19.6-nm laser line completely dominates the spectrum.

two targets are functioning as a quasi-traveling-wave amplifier, and therefore suggests that there is a high output pulse where duration is expected to be about half that of the drive pulse [11].

The estimated uncertainty in this measurement is a factor of 1.5 and is due predominantly to errors in the filter attenuation. Given our best estimates of the source size and the beam divergence (6.6 mrad perpendicular by 30.4 mrad parallel), a lower limit of brightness of 3.0×10^{27} (photons $s^{-1}\,mm^{-2}\,mrad^{-2}$)/$(\Delta\nu/\nu)^{-1}$ is calculated, since we also know the upper limit of the linewidth to be 2.5×10^{-3} nm [20].

The output intensity of the Ge x-ray laser was determined from the experimental data to be 7.9×10^{10} W/cm^2. It is of interest to compare this with the saturated intensity estimated from the Einstein relations between spontaneous and stimulated emission [5]. The collisional depopulation rate of the upper laser level is calculated from complete LASNEX hydrodynamic and kinetic simulations to be 1.15×10^{12} s^{-1} [19]. The linewidth of the 19.6 transition before saturation was measured to be 2.5×10^{-3} nm [20]. In the simulations, typical plasma conditions for the Ge laser were used: an electron temperature of 880 eV, and an electron density of 3×10^{20} cm^{-3}. The saturated intensity is then calculated to be 2.0×10^{10} $W\,cm^{-2}$, which is about a quarter of the measured value.

In conclusion, we have presented output characteristic measurements of a saturated Ne-like Ge x-ray laser. The high brightness and 19.6-nm wavelength of this laser make it an ideal candidate for x-ray laser applications. Recent radiography measurements using this x-ray laser at Rutherford Appleton Laboratory has successfully revealed the modulations due to hydrodynamic imprinting and subsequent Rayleigh-Taylor growth [21].

The authors would like to thank the Vulcan laser operations, the target preparation, and engineering groups of the Central Laser Facility for their help and cooperation. E.W. has been supported by the Austrian Fonds zur Förderung der wissenschaftlichen Forschung under Project No. P10844 NAW. The work of D.K. and J.N. was performed under the auspices of the U.S. Department of Energy by the Lawrence Livermore National Laboratory under Contract No. W-7405-Eng-48.

[1] Y. L. Li, G. Pretzler and E. E. Fill, Phys. Rev. A **52**, R3433 (1995).

[2] D. J. Fields, R. S. Walling, G. M. Shimkaeg, B. J. MacGowan, L. B. Da Siva, J. H. Scofield, A. L. Osterheld, T. W. Phillips, M. D. Rosen, D. L. Matthews, W. H. Goldstein, and R. E. Stewart, Phys. Rev. A **46**, 1606 (1992).

[3] A. Carillon, H. Z. Chen, P. Dhez, L. Dwivedi, J. Jacoby, P. Jaegle, G. Jamelot, J. Zhang, M. H. Key, A. Kidd, A. Klisnick, R. Kodama, J. Krishnan, C. L.S. Lewis, D. Neely, P. Norreys, D. O'Neill, G. J. Pert, S. A. Ramsden, J. P. Raucourt, G. J. Tallents, and J. Uhomoibhi, Phys. Rev. Lett. **68**, 2917 (1992); S. Wang, Y. Gu, S. Fu, G. Zhou, S. Yu, Y. Ni, J. Wu, G. Han, Z. Zhou, B. Wan, Z. Tao, H. Peng, J. Sheng, T. Zhang, Y. Shao, G. Zhang, Z. Lin, S. Wang, W. Chen, and D. Fan, Sci. China A. **34**, 1388 (1991).

[4] J. A. Koch, B. J. MacGowan, L. B. Da Silva, D. L. Matthews, J. H. Underwood, P. J. Batson, and S. Mrowka, Phys. Rev. Lett. **68**, 3291 (1992).

[5] L. B. Da Silva, B. J. MacGowan, S. Mrowka, J. A. Koch, R. A. London, D. L. Matthews, and J. H. Underwood, Opt. Lett. **18**, 1174 (1993).

[6] P. Jaegle, A. Carillon, P. Dhez, P. Goedkindt, G. Jamelot, A. Klisnick, B. Rus, P. Zeitoun, S. Jacquemot, D. Mazataud, A. Mens, and C. Chauvineau, in *X-ray Lasers 1994*, Fourth International Coloquium, Williamsburg, VA, 1994, edited by D. C. Elder and D. L. Matthews, AIP Conf. Proc. No. 332 (AIP, New York, 1994), p. 25.

[7] A. S. Wan, L. B. Da Silva, T. W. Barbee, Jr., R. Cauble, P. Celliers, S. B. Libby, R. A. London, J. C. Moreno, J. E. Trebes, and F. Weber, in *Soft X-Ray Lasers and Applications*, SPIE Proc. Vol. 2520 (SPIE, Bellingham, WA, 1995), p. 97.

[8] J. Nilsen and J. C. Moreno, Phys. Rev. Lett. **74**, 337 (1995).

[9] J. Zhang, S. T. Chunyu, Y. L. You, Q. R. Zhang, S. J. Yang, W. Z. Huang, D. Y. Wu, X. Q. Zhuang, S. P. Liu, Y. Q. Cai, F. Y. Du, X. D. Yuan, X. F. Wei, Y. K. Zhao, H. S. Peng, and J. Nilsen, Phys. Rev. A **53**, 3640 (1996).

[10] D. H. Kalantar, M. H. Key, L. B. Da Silva, S. G. Glendinning, J. P. Knauer, B. A. Remington, F. Weber, and S. V. Weber, Phys. Rev. Lett. **76**, 3574 (1996).

[11] J. C. Moreno, R. C. Cauble, P. Celliers, L. B. Da Silva, J. Nilsen, and A. S. Wan, in *Soft X-Ray Lasers and Applications* (Ref. [7]), p. 97.

[12] G. Cairns, C. L. S. Lewis, A. G. MacPhee, D. Neely, M. Holden, J. Krishnan, G. J. Tallents, M. H. Key, P. N. Norreys, C. G. Smith, J. Zhang, P. B. Holden, G. J. Pert, J. Plowes, and S. A. Ramsden, Appl. Phys. B **58**, 51 (1994).

[13] I. Weaver, Ph.D. thesis, Queen's University of Belfast, Belfast (1996) (unpublished).

[14] B. L. Henke, P. Lee, T. J. Tanaka, R. L. Shimbaukuro, and B. K. Fujikawa, At. Data Nucl. Data Tables **27**, 1 (1982).

[15] J. A. Plowes, G. J. Pert, and P. B. Holden, Opt. Commun. **116**, 260 (1995).

[16] J. C. Moreno, J. Nilsen, Y. Li, P. Lu, and E. E. Fill, Opt. Lett. **21**, 866 (1996).

[17] G. J. Pert (private communication).

[18] A. G. MacPhee, A. Behjat, G. F. Cairns, S. B. Healy, M. H. Key, N. Kim, M. E. Kurkuoglu, M. J. Lamb, C. L. S. Lewis, S. P. McCabe, D. Neely, G. J. Pert, J. Plowes, G. J. Tallents, P. J. Warwick, E. Wolfrum, and J. Zhang (unpublished).

[19] J. Nilsen (private communication).

[20] G. Yuan, Y. Kato, K. Murai, and R. Kodama, J. Appl. Phys. **78**, 3610 (1995).

[21] D. H. Kalantar, L. B. Da Silva, S. G. Glendinning, F. Weber, R. A. Remington, S. V. Weber, M. H. Key, D. Neely, E. Wolfrum, A. Demir, J. Lin, R. Smith, G. J. Tallents, N. S. Kim, J. S. Wark, J. Zhang, C. L. S. Lewis, A. MacPhee, J. Warwick, and J. P. Knauer (unpublished).